Evaluation of Microcanonical Variational Sum of States: Derivation and Application to the Bromobenzene Cation Dissociation Reaction

Jiyoung Oh and Kihyung Song*

Department of Chemistry, Korea National University of Education, Chungbuk 363-791
Received November 11, 1992

A formalism to calculate microcanonical variational transition state theory sum of states, $N(E, R)$, was derived using the Euler angle and spherical polar coordinate systems. This method was applied to the reaction $C_6H_5Br \cdot^+ \to C^6H_5^+ + Br \cdot$. We have an excellent agreement on $N(E, R)$ curves near the transition states between the results calculated either by the Wardlaw and Marcus method or by the present method. Using a simple model potential surface, this reaction showed multiple transition states with the late conversion of the transitional mode. This reaction also showed transition state switching from orbiting (loose) transition state to tight transition state as the reaction energy is increased.

Introduction

Transition state theory (TST)[1-3] usually assumes that the location of transition state (TS) is at the maximum of the minimum energy path (MEP). The rate constant, then, is calculated using the standard RRKM expression,[4-6]

$$k(E) = \frac{N^\ddagger(E-E_0)}{h\rho(E)} \qquad (1)$$

where $N^\ddagger(E-E_0)$ is the sum of states of the TS with available energy equal to $E-E_0$, $\rho(E)$ is the density of states of the reactants with energy E, and E_0 is the activation energy. However, in the case where there is no reverse activation barrier, such as in the simple bond fission reactions, radical-radical and ion-molecule recombinations, and the decomposition reactions of molecular ions, the location of the TS can no longer be determined by the usual way.[7-9] A simple and well-established method is the application of the phase space theory (PST) which assumes that the TS is located at the maximum of the effective potential, and the properties of the TS pertains those of the fragments' rotational and vibrational structures.[10-12] This type of TS's is usually called as an orbiting (or loose) transition state (OTS) representing that the fragments are assumed freely orbiting with respect to each other due to the long distance between them. A package for this kind of calculations is already published.[13]

A more rigorous way to determine the location of the TS would be using the variational criteria.[14-16] In the variational transition state theory (VTST) methods, the reactant density of states is a fixed quantity, and hence the only thing needs to be calculated as a function of the reaction coordinate R is the sum of states in the numerator of Eq. (1). The variational criteria

$$\frac{\partial N(E-V(R);R)}{\partial R} = 0 \qquad (2)$$

where $V(R)$ is the reaction coordinate potential, is then applied to determine the location of the TS.

A number of VTST methods were suggested and used by many people.[7-9,14-27] A flexible transition state theory (FTST) formalism based on the action-angle coordinates has been developed by Wardlaw and Marcus.[7,19-21] This method includes a full implementation of angular momentum coupling between the rotations and orbiting motion of the fragments, as well as total angular momentum conservation. Klippenstein and Marcus derived another expression using Euler angle coordinates.[28,29] For atom-diatom systems, Song and Chesnavich modified the Wardlaw-Marcus method using spherical polar coordinates.[8,9] When only the angular momentum averaged values are necessary to obtain, this method can save a great deal of computing time. Klippenstein suggested a method which can use any internal coordinate such as the dissociating bond length as the reaction coordinate.[25,26] He demonstrated that this method can produce much lower rate constant than conventional center of mass distance reaction coordinates. Smith derived an angular momentum resolved expression by doing the momentum space integral analytically.[24,30]

In this study, the method of Song and Chesnavich is extended using Euler angle coordinates so that it can be applied to the reactions with nonlinear fragments. This method will be applied to the reaction.

$$C_6H_5Br^+ \cdot \to C_6H_5^+ + Br \cdot \qquad (3)$$

which are simple bond cleavage reactions. Previous study on reaction (3) showed that there exist multiple transition state (MTS) at certain conditions.[23] Transition state switching (TSS) from a loose, orbiting transition state (OTS) at low internal energies of the ion, to tight transition state (TTS) at high internal energies was demonstrated at zero angular momentum limit.

TSS may be understood in the following way. As the reactants move along the reaction coordinates, a compromise occurs between two factors-(a) The system available energy decreases as R is extended due to the reaction coordinate potential curve. This causes a decrease in N. (b) The transitional mode frequencies decrease as R is extended due to the change of the motion from bending vibrations to rotations and orbitings. This increases N. At low energies the first factor is the dominant one. Hence the transition state occurs at very large R and is the OTS. At higher energies, the

Microcanonical Variational Sum of States

Bull. Korean Chem. Soc., Vol. 14, No. 3, 1993 405

two factor may offset each other and TSS is expected.

In this study, the sum of states curves for reaction (3) will be obtained without the restriction on angular momentum. In order to achieve the angular momentum averaged $N(E, R)$ curve, the generalized method of Song and Chesnavich[8,9] will be used. The effect of the angular momentum of the final $N(E, R)$ curves are also studied for reaction (3).

The structure of this study is as follows. In Sec. II, the Wardlaw-Marcus method is described for atom-nonlinear fragments. An expression for angular-momentum-averaged $N(E, R)$ calculations for systems with atom-nonlinear fragments is also derived. The results and discussions for reaction (3) are in Sec. III. Conclusive remarks are given in Sec. IV. Appendices are provided for details of the derivation of $N(E, R)$ for linear-nonlinear and nonlinear-nonlinear fragment cases and variable reduction in the Wardlaw-Marcus expression for $J=0$ case.

Theory

Wardlaw-Marcus Method

In the flexible transitions state theory (FTST) method, of Wardlaw-Marcus,[7,19-21] it is assumed that the spectator (*i.e.*, conserved) degrees of freedom are separable from the transitional modes. Given this assumption, the sum of states N (E, J, R) can be expressed as a convolution between the vibrational sum of states of the spectator modes N_v and the angular momentum-conserved density of states of the transitional mode $\rho(\varepsilon, J)$:

$$N(E, J, R) = \int_0^E N_v(E' - \varepsilon)\rho(\varepsilon, J)d\varepsilon, \qquad (4)$$

where $\rho(\varepsilon, J)d\varepsilon$ is the density of states of the transitional modes for the given J, $N_v(E' - \varepsilon)$ is the number of quantum states in the spectator modes, and E' being the available system energy above the zero-point energy E_z. To calculate $\rho(\varepsilon, J)d\varepsilon$ in Eq. (4), two sets of body-fixed coordinate axes are first defined, each fixed in a separating fragment.[20] The origin of each system is located at the center of mass of that fragment, and when either fragment has some symmetry its coordinate axes are chosen to coincide with its symmetry axes. A third set of body fixed coordinates is also defined, fixed in the molecule as a whole. For the coordinates of the transitional modes the action-angle coordinates[20,31] are then introduced.

The material in this section is grouped into three parts: In part 1, a set of action-angle variables suited to atom-nonlinear fragments is obtained. In the second part, the density of transitional states $\rho(\varepsilon, J)$ and the classical Hamiltonian H_{tr} for the transitional modes are expressed in terms of these vairables. Since the potential energy contribution to H_{tr} is modeled in this study to be a function of the atom-nonlinear separation distances as well as the angle between the bromine atom and the benzene ring, a transformation from the action-angle variables to these internal coordinates is given in the last part.

Coordinates. For systems with atom-nonlinear fragments, such as the reaction (3), the following system of coordinates was introduced. This coordinate system is applicable to the systems with atom-nonlinear polyatomic fragment. First, let (x, y, z) denote a set of Cartesian coordinate axes fixed
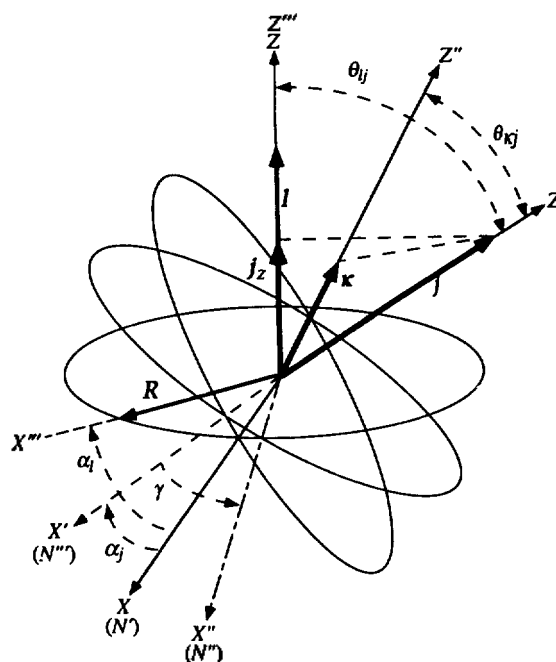

Figure 1. Euler diagram depicting the relationship between the (x, y, z), (x', y', z'), and (x'', y'', z'') Cartesian coordinate systems for the atom-nonlinear polyatomic system. l lies along the z axis, j along the z' axis, and κ is the projection of j on the z'' axis. Pairs of the three xy planes intersect along the lines of nodes N', N'', and N''', whose orientations are determined by the vectors $l \times j$, $l \times \kappa$, $\kappa \times j$, respectively; The angles $(\alpha, \theta_{ij}, 0)$ are the Euler angles specifying the orientation of the primed system relative to the unprimed system, and the angles $(\gamma, \theta_{\kappa j}, 0)$ are those specifying the orientation of the primed system relative to the doubly primed system.

in the $A \cdots X$ system, the z axis being chosen to lie along the relative orbital angular momentum action vector l of the fragments, as in Figure 1. The x axis is chosen to lie along a vector $l \times j$. The relative separation vector R along the line of centers of mass of the two fragments lies in the body-fixed xy plane and is oriented at an angle α_l with respect to the x axis (α_l is conjugate to l).

Two coordinate frames (x', y', z') and (x'', y'', z'') are defined on the fragment X. The atomic position vector r''_{C_6} for C_6 atom of $C_6H_5^+$ is assigned using the $C_6H_5^+$-fixed (x'', y'', z'') Cartesian coordinate system. The double primed axes are chosen to diagonalize the $C_6H_5^+$ inertia tensor. The primed system is chosen so that the z' axes lies along the vector j, and the x' axis lies along the intersection of $x'y'$ and $x''y''$ planes, namely along N''' in Figure 1. The projection of j on the z and z'' axes are denoted by j_z and κ, respectively. The separation vector R''' is chosen to lie along the x''' axis of a (x''', y''', z''') system whose z''' axis coincides with the z axis of the molecule-fixed (x, y, z) system. The origins of the unprimed, singly primed, and triply primed Cartesian systems are chosen to be the center of mass of $C_6H_5^+$. The angles α_l and β_l, which is conjugate angle of l_z, the z projection of l, specify the orientation of the body-fixed (x, y, z) system with respect to a space fixed system. These coordinates provide a set of variables $(l, \alpha_l, l_z, \beta_l, j, \alpha_j, j_z, \beta, \kappa, \gamma)$ which specify the orientation of fragment X in space. Instead
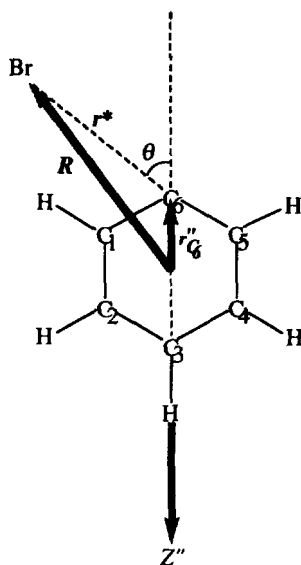
406 *Bull. Korean Chem. Soc., Vol. 14, No. 3, 1993*

Jiyoung Oh and Kihyung Song

Figure 2. Various geometrical variables describing the $C_6H_5Br^+$ system. C_6-Br is the bond being dissociated and r^* is the corresponding "bond" distance. The angle θ and r^* determine the transitional mode potential. R is the vector from $C_6H_5^+$ center of mass to the Br atom and R is the reaction coordinate.

of (I_r, β, j_r, β), the variables (J, a, J_z, β) are used by canonical transformation. The resulting action variables are J, J_z, j, l, and κ, and their respective conjugate angles are $\alpha, \beta, \alpha_t, \alpha_j$, and γ.

Density of Transitional States. The expression for $\rho(\varepsilon, J)$ is

$$\rho(\varepsilon, J) = (2\pi)^{-5}\sigma^{-1} \int \cdots \int dJ_z dj dl d\kappa d\alpha d\beta d\alpha_j d\alpha_l d\gamma$$

$$\times \Delta(J, j, l) \, \delta(\varepsilon - H_d) \tag{5}$$

for a given value of J. The limits on the angle variables are 0 to 2π. The J_z integral is over the integral $(-J, J)$, and the κ integral is restricted by $|\kappa| \leq j$. σ is a symmetry number which corrects for the overcounting of any indistinguishable configurations in these $(0, 2\pi)$ angle intervals. $\Delta(J, j, l)$ is unity when the triangle inequality $|j-l| \leq J \leq j+l$ is fulfilled and zero otherwise. The Hamiltonian H_d for the transitional mode is written as

$$H_d = E_r + \frac{l^2}{2\mu R^2} + V_t(r^*, \theta), \tag{6}$$

where μ is the reduced mass for relative motion of $C_6H_5^+$ and $Br \cdot$, E_r is the rotational energy of the $C_6H_5^+$ fragment, and V_t is the potential energy function for the transitional modes. The arguments of V_t in Eq. (6) are given as follows: r^* is the distance from C_6 atom to the dissociating Br atom, and θ is the angle between r^* and the line passing through the two points, C_6 and center of benzene ring, as shown in Figure 2. When the fragment X is a symmetric top, its rotational energy E_r of a fragment X has the form $j^2/2I_A + \kappa^2/2I_r$, where $I_r = I_A I_C/(I_A - I_C)$. The principal moments of inertia (I_A, I_B, I_C) of a fragment are determined from its equilibrium geometry. In the case of $C_6H_5^+$ fragments, I_A and I_B are almost equal. Hence, $C_6H_5^+$ is considered as an oblate sym-

metric top with $I_A = I_B < I_C$, which yields $I_r < 0$.

Internal Coordinates. The internal coordinater r^* and θ, in which the transitional mode potential V_t is expressed, are determined from the action-angle coordinates as follows. By transforming R''' and r''_{C_6} to the (x, y, z) system, the coordinates r^*, and θ are obtained by

$$r^* = |R - r_{C_6}|,$$

$$\cos(\pi - \theta) = \frac{r^2_{C_6} + r^{*2} - R^2}{2r_{C_6}r^*}.$$

For given R, J, and six-dimension Monte Carlo point $(l, j, \kappa, \alpha_l, \alpha_j, \gamma)$ the vectors R and r_{C_6} are obtained by application of the inverse rotation matrix A^{-1}.[31]

$$r_{C_6} = A^{-1}(\alpha_j, \theta_{lj}, 0)A^{-1}(\gamma, \theta_{\kappa j}, 0)r''_{C_6}. \tag{7}$$

$$R = A^{-1}(\alpha_l, 0, 0)R'''. \tag{8}$$

The first application of A^{-1} in Eq. (7) yields the intermediate vector r' in a $C_6H_5^+$-fixed (x', y', z') system whose z' axis lies along j. This primed coordinates are rotationally related to the (x'', y'', z'') system by the Euler angles $(\gamma, \theta_{\kappa j}, 0)$. The angle γ (conjugate to κ) is the angle between the x'' and x' axes. The x' axis is lying along the line of nodes $\kappa \times j$. $\theta_{\kappa j} = \cos^{-1}(\kappa/j)$ is the angle contained between the vectors κ and j (i.e., between the z'' and z' axes). The second set of Euler angles $(\alpha_j, \theta_{lj}, 0)$ in Eq. (7) connects the (x', y', z') and (x, y, z) systems: α_j (conjugate to j) is the angle between the x' and x axes, the latter lying along the line of nodes $l \times j$; $\theta_{lj} = \cos^{-1}((j^2 - l^2 - j^2)/2lj)$ is the angle contained between the vector l and j (i.e., between the z' axis and the z axis). The Euler angle α_l in Eq. (8) is conjugate to l and is the angle between the x''' and x axes. H_d is specified by the variables $(R, J, l, j, \kappa, \alpha_l, \alpha_j, \gamma)$ and is independent of (J_z, α, β). Eq. (5) now becomes

$$\rho(\varepsilon, J) = (2J+1)(2\pi)^{-3}\sigma^{-1} \int \cdots \int dj dl d\kappa d\alpha_j d\alpha_l d\gamma$$

$$\times \Delta(J, j, l) \, \delta(\varepsilon - H_d) \tag{9}$$

and

$$N(E, J, R) = (2J+1)(2\pi)^{-3}\sigma^{-1} \int \cdots \int dj dl d\kappa d\alpha_j d\alpha_l d\gamma$$

$$\times N_v(E' - H_d)\Delta(J, j, l) \tag{10}$$

This is the equation used to evaluate $N(E, J, R)$ for atom-nonlinear polyatomic fragment systems using the FTST method of Wardlaw and Marcus.[7,19-21] Since the evaluation of this equation requires a six-fold integration with boundary conditions that can often be quite complex, the integration are usually carried out using Monte Carlo techniques. A detailed derivation for the case of $J = 0$ is described in Appedix A.

The angular momentum averaged $N(E, R)$ values can also be obtained by integrating Eq. (10) over J, i.e.,

$$N(E, R) = \int dl \, N(E, J, R). \tag{11}$$

The integration over J was done using the following points.

$$0, 10, 20, 50, 100, 200, \cdots, 700, J^{\ddagger}$$

where $J^{\ddagger}$ is the integration limit described elsewhere.[9]

Direct Calculation of $N(E, R)$

Given the FTST equations summarized above, the evaluation of the angular momentum averaged microcanonical variational sum of states $N(E, R)$ can be carried out directly in the following manner: First, the quantity $\rho(\varepsilon)$, the rotational density of states summed over the total angular momentum J, can be obtained from Eq. (5) by integrating over J.[7,19-21]

$$\rho(\varepsilon) = \frac{1}{(2\pi)^5 \sigma} \int \cdots \int dJ dJ_z dj dl d\kappa d\alpha d\beta d\alpha_j d\alpha_l d\gamma$$

$$\times \Delta(J, j, l)\ \delta(\varepsilon - H_{tr}) \quad (12)$$

Note that this integration covers the entire rotational-orbital phase space of the atom-nonlinear polyatomic fragment system. Hence it can be rewritten using phase space volume elements $d\tau_j$ as[8,3]

$$\rho(\varepsilon) = \sigma^{-1} \int d\tau_1 d\tau_2 \delta(\varepsilon - H_{tr}). \quad (13)$$

The $d\tau_j$ can be written in terms of the action-angle coordinate system used in Eq. (12), or in terms of spherical-polar coordinates for atom-linear fragments.[8,32] For an atom-nonlinear polyatomic fragment system, the transitional mode Homiltonian H_{tr} can be written, using Euler angle coordinates,[24,28-31,33] as

$$H_{tr} = B_l l^2 + B_a P_a^2 + B_b P_b^2 + B_c P_c^2 + V_t(R, \theta, \phi) \quad (14)$$

where B_l is the orbiting rotation constant for atom-nonlinear pair, B_a, B_b, and B_c are the rotational constants for nonlinear fragment around the principal axes, P_a, P_b, and P_b, are the angular momentum components for the principal axes, R is the reaction coordinate, θ is the angle between symmetry axis and reaction coordinate, and ϕ is the rotation angle about symmetry axis. In spherical-polar coordinates, the orbiting angular momentum l is defined by

$$l^2 = p^2_{\theta_1} + \frac{p^2_{\phi_1}}{\sin^2 \theta_1}. \quad (15)$$

Using the spherical polar coordinates given in Eq. (15), the differential volume element $d\tau_1$ can be written as

$$d\tau_1 = (2\pi)^{-2} \sin \theta_1 dp_{\theta_1} dp_{\phi_1} d\theta_1 d\phi_1. \quad (16)$$

For the rotation of the nonlinear fragments, $d\tau_2$ can be written using the Euler angle coordinates, as

$$d\tau_2 = (2\pi)^{-3} \sin \theta_2 dp_{\theta_2} dp_{\phi_2} dp_{\psi_2} d\theta_2 d\phi_2 d\psi_2. \quad (17)$$

The limits of integration over the angles θ_2, ϕ_2, and ψ_2 are $0-\pi$, $0-2\pi$, and $0-2\pi$, respectively. The transformation from the Euler axes momenta to the principal axes momenta can be performed with $J_c = 1$.[24]

$$\{d_{\theta_2}, p_{\phi_2}, p_{\psi_2}\} \xrightarrow{J_c = 1} \{p_a, p_b, p_c\} \quad (18)$$

Using the properties of the δ-function, the simplification of Eq. (16) can be performed as follows.[8,32] First, let $p_{\theta_1} = l$, $p_{\phi_1} = 0$, and $\theta_1 = 0$, i.e., place the particle initially on the space-fixed z axis. The angle ϕ_1 can be chosen arbitrarily. It is necessary to perform the integration

$$\int d\tau_1 \delta[l - l(p_{\theta_1}, p_{\phi_1}, \theta_1)] = \frac{d}{dl} \int d\tau_1\, h[l - l(p_{\theta_1}, p_{\phi_1}, \theta_1)] \quad (19)$$

to produce $d\tau_1$. Here, $h(x)$ is a hemisidal step function. The

integration on the right-hand side can be written explicitly as

$$\int h\tau_1 \delta[l - l(p_{\theta_1}, p_{\phi_1}, \theta_1)] =$$

$$(2\pi)^{-2} \int_0^\pi \sin\theta_1 d\theta_1 \int_0^{2\pi} d\phi_1 \int_{-\infty}^\infty dp_{\theta_1} \int_{-\infty}^\infty dp_{\phi_1}$$

$$\times h\left[l - \left(p_{\theta_1}^2 + \frac{p_{\phi_1}^2}{\sin^2\theta_1}\right)^{\frac{1}{2}}\right] \quad (20)$$

Here, the integration over p_{θ_1} and p_{θ_1} is equal to the area of the ellipse of Eq. (15) which is equal to $\pi l^2 \sin \theta_1$. The integration over ϕ_1 yields 2π and the integration over θ_1 yields 2 because of the factor $\sin \theta_1$. The result of Eq. (20) becomes l^2. By differentiating this over l, Eq. (19) yields $2l$. Hence, $d\tau_1$ becomes

$$d\tau_1 = 2l dl. \quad (21)$$

Inserting Eqs. (14), (17), (18), and (21) to Eq. (13) yields

$$\rho(\varepsilon) = \sigma^{-1} (2\pi)^{-3} \int 2l dl\ \sin\theta_2 dp_a dp_b dp_c d\theta_2 d\phi_2 d\psi_2 \delta(\varepsilon - H_{tr}). (22)$$

The angle ψ_2 can be integrated since the configuration of the system can be defined with the two angles, θ_2 and ϕ_2. This integration yields 2π. Eq. (4) now becomes the convolution integral between the vibrational sum of, states and rotational-orbital density of states:

$$N(E, R) = \frac{1}{(2\pi)^2 \sigma} \int_0^E d\varepsilon \int_0^\pi \sin\theta_2 d\theta_2 \int_0^{2\pi} d\phi_2 N_v[E - \varepsilon - V_t(R, \theta, \phi)]$$

$$\times \int dp_a dp_b dp_c \int 2l dl\ \delta[\varepsilon - (B_l l^2 + B_a P_a^2 + B_b P_b^2 + B_c P_c^2)] \quad (23)$$

Integration over the momenta, l, p_a, p_b, and p_c can be done by the Dirichlet Integral.[34] This yields

$$\int dp_a dp_b dp_c \int 2l dl\ \delta[\varepsilon - (B_l l^2 + B_a P_a^2 + B_b P_b^2 + B_c P_c^2)]$$

$$= \frac{4\pi}{3B_l \sqrt{B_a B_b B_c}}\ \varepsilon^{3/2}. \quad (24)$$

Inserting Eq. (24) to Eq. (23) yields final equation for the microcanonical sum of states

$$N(E, R) = \frac{1}{3\pi\sigma B_l \sqrt{B_a B_b B_c}} \int_0^E d\varepsilon\ \varepsilon^{3/2}$$

$$\int_0^\pi \sin\theta_2 d\theta_2 \int_0^{2\pi} d\phi_2 N_v[E - \varepsilon - V_t(R, \theta, \phi)]. \quad (25)$$

For systems other than atom-nonlinear pair, detailed derivations are given in the Appendix B.

Results and Discussions

The microcanonical variational sum of states curves are calculated for reaction (3) using both methods described above. The same potential surface is used as in the previous study.[23] In Figure 3 the $N(E, R)$ values obtained by Eq. (25) are compared to the results using Eqs. (10) and (11) with integration limit $J^{\ddagger}$. Two results are in excellent agreement except at extremely large R. Considering the two to three orders of magnitude difference in the computing time between Eqs. (11) and (25), these results suggest that it is
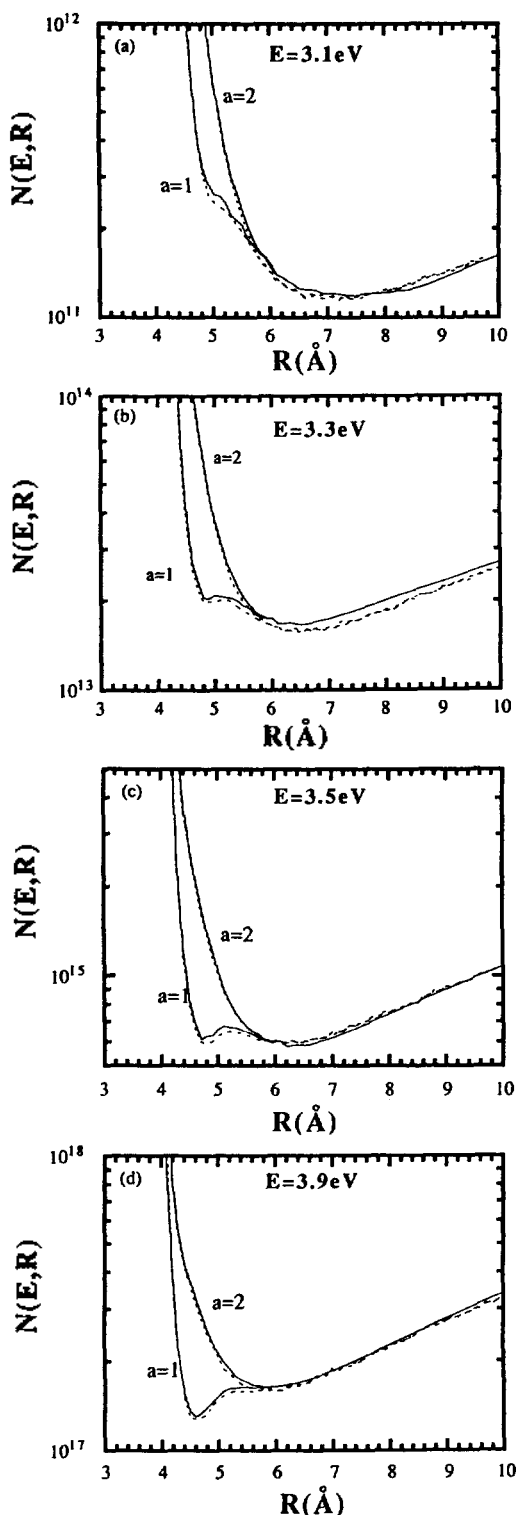
Figure 3. $N(E, R)$ curves for $C_6H_5Br^+$·system. Solid lines are the results of Eq. (25), the direct calculation of $N(E, R)$. The dotted line represent the results of Eq. (10) using the J^t values.

much more efficient to use Eq. (25) when it is not necessary to study the effect of the angular momentum.

Two transition states were observed for a late loosening of the transitional modes ($a = 1$) as the energy increases, one at a small internuclear distance and one at large inter-

nuclear distance. The simultaneous existence of multiple transition states is observed with system energies between 3.3 eV and 3.9 eV. The transition state switching (TSS) from OTS to TTS occurs around $E = 3.5$ eV as shown in Figure 3(c).

With early loosening of the transitional modes ($a = 2$), however, there exists only one TS and the OTS is the dominant transition state at energies studied in this research. It is due to the fact that the conversion of the transitional modes from bending vibration to rotation and orbiting is rapid due to early decrease of rotational hindrance as the reaction coordinate is extended. In a late loosening of the transitional modes ($a = 1$), the conversion from motion of bending vibration to rotation and orbiting is slow due to slow decrease of rotational barrier as the reaction coordinate extended. This decreases sum of states significantly in the region of the small internuclear distance compared to the early loosening of the transitional mode ($a = 2$) case. This is the reason why this system yields TTS at a small internuclear distance with late conversion.

We have also carried out same procedure for loosening parameter $a = 1.5$ which have not been shown here. The result of parameter $a = 1.5$ always showed the average behavior of two previous results *i.e.*, $a = 1$ and $a = 2$.

The $N(E, J, R)$ curves for a various values of J are shown in Figure 4. At $E = 3.1$ eV, the $N(E, J, R)$ curves show that OTS is slightly dominant for all J values except $J = 300$. At $E = 3.3$ eV, as shown in Figure 4(b), the TTS was preponderant for J above 200, while, at below this J value the OTS gave a slightly larger value for the sum of states. Figure 4(c) shows the $N(E, J, R)$ curves at $E = 3.9$ eV. At this energy, the TTS was prevalent for J values above 200, while, at below this J value, the OTS gave a slightly larger value for the sum of states. Due to the $(2J + 1)$ factor in Eq. (10), the shape of $N(E, J, R)$ curves at large J determines the behavior of $N(E, R)$ curves. These results support the fact that the OTS is dominant at $E = 3.1$ eV, the TTS is emerging at $E = 3.3$ eV, and the TTS is the only transition state at $E = 3.9$ eV.

Conclusions and Remarks

In this study, the $N(E, J, R)$ curves were calculated using the original FTST method of Wardlaw and Marcus, Eq. (10). The angular momentum averaged results of $N(E, R)$ curves obtained from Eq. (11) were compared to the results using Eq. (25) which was derived using the spherical polar coordinates for orbiting motion and the Euler angle coordinates for fragment rotations. The agreement between the two methods was excellent.

The individual $N(E, J, R)$ curves support the behavior of the angular momentum averaged $N(E, R)$ curves. An interesting fact should be noted is that, due to $(2J + 1)$ factor in Eq. (10), the high-J curves have more effect on the final $N(E, R)$ curve.

Microcanonical VTST calculations for the dissociation reaction of bromobenzene cation demonstrate the existence of multiple transition states. Late loosening of the transitional modes leads to MTS at internal energy as low at $E = 3.3$ eV and exhibits TSS as the energy increases. With a loosening parameter $a = 2$, there is only one TS which is the
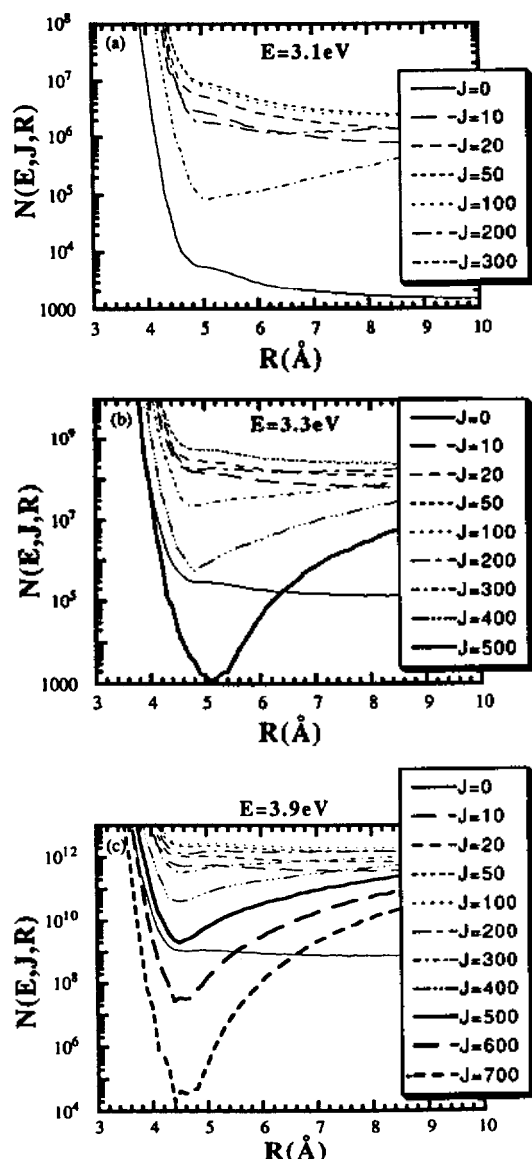
Microcanonical Variational Sum of States

Bull. Korean Chem. Soc., Vol. 14, No. 3, 1993 409

Figure 4. The effect of angular momentum of the $C_6H_5Br^+ \cdot$ system.
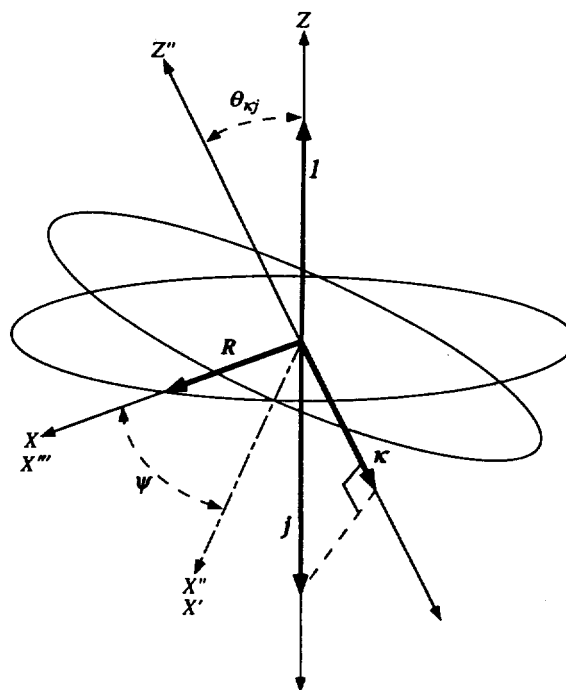

Figure 5. Euler diagram depiciting the relationship between the (x, y, z) and (x', y', z') Cartesian coordinate systems for the atom-nonlinear polyatomic system at $J=0$. l lies along the z axis, j along the opposite direction, and κ is the projection of j on the z'' axis. Pairs of the two xy planes intersect along the lines of nodes N'' whose orientations are determined by the vectors $l \times \kappa$. ψ is equal to $2\theta_s$.

OTS.

Appendix

A. Variable Reduction for $J=0$ Case

If $J=0$, then $l=-j$, and $\cos \theta_{lj}=-1$. That is the Δ in Eq. (11) becomes $\delta(j-l)$. The reference axis $l \times j$ for α_l and α_j is no longer defined. Euler diagram for the atom-nonlinear polyatomic system in the zero angular momentum limit was given in Figure 5. Writing $\theta_s=(\alpha_l+\alpha_j)/2$, $\theta_d=\alpha_l-\alpha_j$, and introducing the function $\delta(j-l)$ in Eq. (5), a six-dimensional integral is obtained.

$$\rho_{J=0}(\varepsilon) = (2\pi)^{-3}\sigma^{-1}\int \cdots \int dj dl d\kappa d\Upsilon \int_0^\pi d\theta_s \int_0^\pi d\theta_d \delta(j-l)\delta(\varepsilon-H_d).$$

(A1)

After integrating over l and θ_d, one obtains

$$\rho_{J=0}(\varepsilon) = (2\pi)^{-3}\sigma^{-1}\int \int \int dj d\kappa d\Upsilon \int_0^\pi d\theta_s \delta(\varepsilon-H_d).$$

(A2)

Inserting Eq. (A2) into Eq. (4) yields the final equation

$$N(E, 0, R) = 2^{-1}(2\pi)^{-2}\sigma^{-1}\int \int \int dj d\kappa d\Upsilon \int_0^\pi d\theta_s N_v(E'-H_d).$$

(A3)

B. Expressions for Linear-Nonlinear and Nonlinear-Nonlinear Cases

For linear-nonlinear system, the Hamiltonian Can be written as

$$H=B_j l^2 + B_j j^2 + B_a P_a^2 + B_b P_b^2 + B_c P_c^2 + V_t(R, \theta, \phi, \psi, \theta_l)$$

(B1)

where ψ is the rotation angle of the nonlinear fragment around R, and θ_l is the rotation angle of the linear fragment around R. In spherical-polar coordinates, the differential volume element $d\tau$ for the transitional modes is given by

$$d\tau = d\tau_1 d\tau_2 d\tau_3$$

(B2)

where $d\tau_1$ is for the orbiting motion, $d\tau_2$ is for the linear rotor, and $d\tau_3$ is for the nonlinear rotor, respectively. They can be written by[8,32]

$$d\tau_1 = 2l dl,$$

(B3a)

$$d\tau_2 = \frac{2j dj \sin\theta_l d\theta_l}{2}$$

(B3b)

$$d\tau_3 = \frac{\sin\theta dp_a dp_b dp_c d\theta d\phi d\psi}{(2\pi)^3}$$

(B3c)

Inserting Eqs (B3a), (B3b), and (B3c) to Eq. (12) yields the following convolution integral between the vibrational sum of states and rotational-orbital density of states:

$$N(E, R) = \frac{1}{2(2\pi)^3} \int_0^E dE_r \int_0^\pi \sin\theta_l d\theta_l \int_0^\pi \sin\theta d\theta \int_0^{2\pi} d\phi \int_0^{2\pi} d\psi$$

$$\times N_v[E - E_r - V_l(R, \theta, \phi, \psi, \theta_l)] \int dP_a dP_b dP_c \int 2l dl \int 2j dj$$

$$\times \delta[E_r - (B_l l^2 + B_j)^2 + B_a P_a^2 + B_b P_b^2 + B_c P_c^2)] \tag{B4}$$

where E_r is equal to the rotational energy of the system. Here we use Dirichlet Integral[34] for evaluating the momentum integral below.

$$\int dP_a dP_b dP_c \int 2l dl \int 2j dj \, \delta[B_l l^2 + B_j j^2 + B_a P_a^2 + B_b P_b^2 + B_c P_c^2]$$

$$= \frac{8\pi}{15 B_l B_j \sqrt{B_a B_b B_c}} E_r^{5/2} \tag{B5}$$

Inserting Eq. (B5) to Eq. (B4) and performing integration of ψ yields the final equation for the linear-nonlinear par.

$$N(E, R) = \frac{1}{2(2\pi)^3} \frac{8\pi}{15 B_l B_j \sqrt{B_a B_b B_c}} \int_0^E dE_r E_r^{5/2} \int_0^\pi \sin\theta_l d\theta_l$$

$$\times \int_0^\pi \sin\theta d\theta \int_0^{2\pi} d\phi \int_0^{2\pi} d\psi N_v[E - E_r - V_l(R, \theta, \phi, \psi, \theta_l)] \tag{B6}$$

where $B_l B_j$ and $B_a B_b B_c$ are rotational constants.

For nonlinear-nonlinear system, the Hamiltonian can be written as

$$H = B_l l^2 + B_{a1} P_{a1}^2 + B_{b1} P_{b1}^2 + B_{c1} P_{c1}^2$$

$$+ B_{a2} P_{a2}^2 + B_{b2} P_{b2}^2 + B_{c2} P_{c2}^2 + V_l(R, \theta_1, \phi_1, \psi_1, \theta_2, \phi_2). \tag{B7}$$

The orbiting motion volume element $d\tau_1$ is given by Eq. (B3). The rotational volume elements for two nonlinear rotors are given using the Euler angles by

$$d\tau_j = \frac{\sin\theta_i dP_{a_i} dP_{b_i} dP_{c_i} d\theta_i d\phi_i d\psi_i}{(2\pi)^3}, \quad j = 2, 3 \tag{B8}$$

Inserting Eqs. (B3) and (B8) into Eq. (12) yields

$$N(E, R) = \frac{1}{2(2\pi)^5} \int_0^E dE_r \int_0^\pi \sin\theta_l d\theta_l$$

$$\int_0^\pi \sin\theta_{2l} d\theta_2 \int_0^{2\pi} d\phi_1 \int_0^{2\pi} d\phi_2 \int_0^{2\pi} d\psi_1$$

$$\times N_v[E - E_r - V_l] \int dP_{a1} dP_{b1} dP_{c1} dP_{a2} dP_{b2} dP_{c2} \int 2l dl$$

$$\times \delta[E_r - (B_l l^2 + B_{a1} P_{a1}^2 + B_{b1} P_{b1}^2 + \cdots + B_{c2} P_{c2}^2)] \tag{B9}$$

where E_r is equal to the rotational energy of the system. Applying Dirichlet integral to the following momentum integral

$$\int dP_{a1} dP_{b1} dP_{c1} dP_{a2} dP_{b2} dP_{c2} \int 2l dl$$

$$\times \delta[E_r - (B_l l^2 + B_{a1} P_{a1}^2 + B_{b1} P_{b1}^2 + \cdots + B_{c2} P_{c2}^2)].$$

$$= \frac{\pi^3}{6 B_l \sqrt{B_{a1} B_{b1} \cdots B_{c2}}} E_r^3 \tag{B10}$$

Inserting Eq. (B10) to Eq. (B9) and performing integration of ψ_2 yields the final equation.

$$N(E, R) = \frac{1}{2(2\pi)^5} \frac{\pi^3}{6 B_l \sqrt{B_{a1} B_{b1} \cdots B_{c1}}} \int_0^E dE_r E_r^3 \int_0^\pi \sin\theta_l d\theta_l$$

$$\times \int_0^\pi \sin\theta_2 d\theta_2 \int_0^{2\pi} d\phi_1 \int_0^{2\pi} d\phi_2 \int_0^{2\pi} d\psi_1 N_v(E - E_r - V_l) \tag{B11}$$

where B_l and $B_{a1} B_{b1} \cdots B_{c2}$ are rotational constants.

References

1. M. G. Evans and M. Polyanyi, *Trans. Faraday Soc.*, **31**, 875 (1935).
2. H. Eyring, *J. Chem. Phys.*, **3**, 107 (1935).
3. H. Eyring and W. F. K. Wynne-Jones, *J. Chem. Phys.*, **3**, 492 (1935).
4. R. A. Marcus and O. K. Rice, *J. Phys. Colloid Chem.*, **55**, 894 (1951).
5. R. A. Marcus, *J. Chem. Phys.*, **20**, 4658 (1952).
6. H. M. Rosenstock, M. B. Wallenstein, A. L. Wahrhaftig, and H. Eyring, *Proc. Natl. Acad. Sci. U.S.A.*, **38**, 667 (1952).
7. D. M. Wardlaw and R. A. Marcus, *Adv. Chem. Phys.*, **70**, 231 (1988).
8. K. Song and W. J. Chesnavich, *J. Chem. Phys.*, **91**, 4664 (1989).
9. K. Song and W. J. Chesnavich, *J. Chem. Phys.*, **93**, 5751 (1990).
10. W. J. Chesnavich and M. T. Bowers, *Prog. React. Kinet.*, **11**, 137 (1982).
11. M. E. Grice, K. Song, and W. J. Chesnavich, *J. Phys. Chem.*, **90**, 3503 (1986).
12. I.-C. Chen, W. H. Green Jr., and C. B. Moore, *J. Chem. Phys.*, **89**, 314 (1988).
13. W. J. Chesnavich, L. Bass, M. E. Grice, K. Song, and D. A. Webb, *Q.C.P.E.*, **8**, 557 (1988).
14. W. L. Hase, *Acc. Chem. Res.*, **16**, 258 (1983).
15. D. G. Truhlar and B. C. Garrett, *Ann. Rev. Phys. Chem.*, **35**, 159 (1984).
16. D. G. Truhlar A. D. Isaacson, and B. C. Garrett, in *Theory of Chemical Reaction Dynamics*, Vol. IV, edited by M. Baer (CRC Press, Boca Raton, Florida, 1985), p. 65.
17. W. J. Chesnavich, *J. Chem. Phys.*, **84**, 2615 (1986).
18. S. N. Rai and D. G. Truhlar, *J. Chem. Phys.*, **79**, 6046 (1983).
19. D. M. Wardlaw and R. A. Marcus, *Chem. Phys. Lett.*, **110**, 230 (1984).
20. D. M. Wardlaw and R. A. Marcus, *J. Chem. Phys.*, **83**, 3462 (1985).
21. D. M. Wardlaw and R. A. Marcus, *J. Phys. Chem.*, **90**, 5383 (1986).
22. G. W. Koeppl, *J. Chem. Phys.*, **87**, 5746 (1987).
23. C. Lifshitz, F. Louage, V. Aviyente, and K. Song, *J. Phys. Chem.*, **95**, 9298 (1991).
24. S. C. Smith, *J. Chem. Phys.*, **95**, 3404 (1991).
25. S. J. Klippenstein, *Chem. Phys. Lett.*, **170**, 71 (1990).
26. S. J. Klippenstein, *J. Chem. Phys.*, **94**, 6469 (1991).
27. S. J. Klippenstein, *J. Chem. Phys.*, **97**, 2406 (1992).
28. S. J. Klippenstein and R. A. Marcus, *J. Phys. Chem.*, **92**,

3105 (1988).

29. S. J. Klippenstein and R. A. Marcus, *J. Phys. Chem.*, **92**, 5412 (1988).

30. S. C. Smith, *J. Chem. Phys.*, **97**, 2406 (1992).

31. H. Goldstein, *Classical Mechanics, 2nd.* ed. (Addison-Wesley, Reading, MA, 1980).

32. K. Song, Ph. D. Dissertation, Texas Tech University, 1989.

33. E. E. Aubanel and D. M. Wardlaw, *J. Phys. Chem.*, **93**, 3117 (1989).

34. R. C. Tolman, *The Principles of Statistical Mechanics* (Dover, New York, 1979).